---

**Article:**
Xu, Huixian, Li, Yan-Jun, Li, Qin et al. (7 more authors) (2023) Reactive oxygen species induced by plant essential oil for effective degradation of p-phenylenediamine. Green Chemistry. ISSN 1463-9270

https://doi.org/10.1039/D3GC00707C

---

View Article Online
View Journal

# Green Chemistry

Cutting-edge research for a greener sustainable future

## Accepted Manuscript

This article can be cited before page numbers have been issued, to do this please use: H. Xu, Y. Li, Q. Li, D. Yang, T. Li, S. Jin, L. Zhou, Q. Zhang and J. H. Clark, *Green Chem.*, 2023, DOI: 10.1039/D3GC00707C.

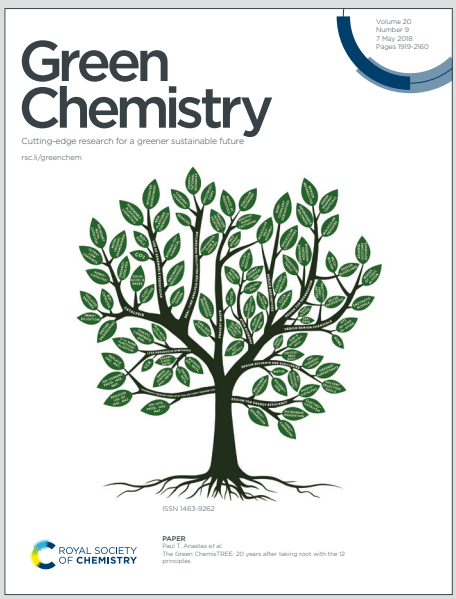

View Article Online
DOI: 10.1039/D3GC00707C

ARTICLE

# Reactive oxygen species induced by plant essential oil for effective degradation of *p*-phenylenediamine †

Received 00th January 20xx,
Accepted 00th January 20xx

DOI: 10.1039/x0xx00000x

Huixian Xu,‡[a] Yanjun Li,‡[a] Qin Li,[a] Dandan Yang,[a] Ting Li,[a] Saimeng Jin,*[a] Liandi Zhou,*[b] Qihui Zhang*[a] and James H. Clark[c]

*p*-Phenylenediamine (PPD) is an aromatic amine commonly used in hair dyes which has high toxicity including carcinogenicity and mutagenicity. It is crucial to eliminate its danger to public health and environmental quality. Advanced oxidation processes (AOPs) are promising methods to degrade contaminants using reactive oxygen species (ROS) but are often complex and toxic. Herein, a simple, green and environmentally friendly strategy is proposed to degrade pollutants using biochar loaded with self-emulsifying orange peel essential oil (BC/SE-OPEO) to efficiently adsorb and degrade PPD. After the optimal experiments, the results show that the PPD removal efficiency of 50 mg BC/SE-OPEO reaches around 98% after 110 min at 40 °C. In addition, BC/SE-OPEO was successfully applied to the removal of PPD from actual hair dye sewage and from dyed hair. Mechanistic investigations prove that ROS plays a vital role in the degradation of PPD which is eventually degraded to carbon dioxide and water.

## Introduction

Hair dyes are widely used in the beauty industry. *p*-Phenylenediamine (PPD) is a type of aromatic amine in commercial hair dye, but PPD has high toxicity notably carcinogenicity and mutagenicity.[1-4] The solubility of PPD in water is 47,000 mg/L, resulting in its accumulation in environmental water after use. The European Commission has included PPD in its list of 22 prohibited compounds. In the 2015 edition "Technical Specifications for Cosmetic Safety", China has stipulated that the maximum allowable concentration of PPD in hair dye is 2%. The Environmental Protection Agency of the United States has regulated that the maximum acceptable concentration of PPD in the ambient air of the workshop is 0.1 mg/m$^3$. Prolonged and repeated exposure to PPD can cause allergy, asthma, gastritis, kidney failure and other serious diseases.[5-7] Given the popularity of hair dying and the lack of cost-effective alternatives, it is important to explore efficient method to degrade PPD.

Advanced oxidation processes (AOPs) are commonly employed to decompose organic pollutants into harmless small molecules, such as carbon dioxide and water by generating reactive oxygen species (ROS).[8] Degradation of pollutants based on varieties of AOPs such as ozone, photocatalysis, ultrasound, ultraviolet and electrochemical methods have been reported. Asgari *et al*. synthesized magnesium oxide magnetic nanoparticles to remove aniline from aqueous solution by ozonation and catalytic ozonation.[9] Chen *et al*. prepared titanium dioxide-coated magnetic poly (methyl methacrylate) microspheres for PPD photocatalytic degradation.[10] Qiao *et al*. prepared Fe-Mn oxides composite as a heterogeneous peroxydisulfate catalyst for aniline degradation.[11] However, due to the complexity and toxicity of the above methods, it is necessary to find a simpler and more environmentally friendly method to degrade contaminants. It has been reported that herb volatile constituents can promote the production of ROS, which enables the degradation of polypropylene plastics.[12] Sunohara *et al*. found that the growth inhibition of onion root induced by cuminaldehyde is due to ROS overproduction.[13] Ahuja *et al*. explored that eugenol inhibits root growth in *Avena fatua* by inducing ROS.[14] Dahiya *et al*. investigated that *Pogostemon* oil promotes the generation of ROS leading to oxidative stress.[15] Ao *et al*. found that the presence of large quantities of limonene in essential oils can promote the production of singlet molecular oxygen, resulting in high cytotoxicity.[16] Overall, the ROS induced by plant essential oils to degrade pollutants is interesting, worthy of further research and with real commercial potential.

Herein, orange peel essential oil (OPEO) was selected to promote the production of ROS. Orange peel is a very large volume and globally available waste from the production of orange juice. Surfactant and co-surfactant were added into the OPEO to prepare the self-emulsifying OPEO (SE-OPEO). Biochar (BC) obtained by pyrolysis of orange peel was then added as a carrier to adsorb SE-OPEO to form BC loaded with SE-OPEO

[a] School of Chemistry and Chemical Engineering, Chongqing University, Chongqing, 400044, China. E-mail: sj708@cqu.edu.cn (S. Jin), qhzhang@cqu.edu.cn (Q. Zhang)
[b] Chongqing College of Traditional Chinese Medicine, Chongqing 402760, China. E-mail: zhouliandi@cqctcm.edu.cn (L. Zhou)
[c] Circa Renewable Chemistry Institute, Green Chemistry Centre of Excellence, University of York, York, YO10 5DD, UK and Shanghai Institute of Pollution Control and Ecological Security, Shanghai, 200092, China.
† Electronic Supplementary Information (ESI) available: Supporting experimental procedures, supporting figures, supporting tables. See DOI: 10.1039/x0xx00000x
‡ These authors contributed equally to this work.

(BC/SE-OPEO), which can adsorb and degrade PPD in hair dye sewage and dyed hair simultaneously. This research demonstrates the feasibility of degrading pollutants by employing plant essential oils to promote the generation of ROS, and proposes a new vision which making use of waste orange peels for contaminants disposal. Thus a waste is usefully employed to tackle a real environmental problem.

## Results and discussion

### Preparation of materials

The preparation of BC/SE-OPEO is shown in **Scheme 1**. Self-emulsifying formulation generally composes of oil, surfactant, co-surfactant and active ingredient. OPEO can be used as both oil and active ingredient. The choice of surfactant and co-surfactant has a great influence on the self-emulsifying efficiency of the formulation. When different formulations are added to the aqueous phase, they will self-emulsify to form different states of oil-in-water emulsions. Some common surfactants and co-surfactants that are miscible with OPEO without stratification or precipitation were selected to prepare several different self-emulsifying formulations, and their self-emulsifying efficiency was visually evaluated (**Table 1**). It was observed that the optimal surfactant and co-surfactant is Triton X-100 and isopropyl alcohol (IPA) respectively, with visual grade reach grade A, as well as giving the highest self-emulsifying efficiency. We thereafter used for our degradation studies a SE-OPEO composition of OPEO, Triton X-100 and IPA.

The pseudo-ternary phase diagram for OPEO, Triton X-100 and IPA is illustrated in **Fig. 1**. The shaded region indicates that the formulations can self-emulsify effectively to form an emulsion and only formulations with OPEO concentration no more than 25% have self-emulsifying ability. Therefore, the mass fractions of OPEO, Triton X-100 and IPA are determined to be in the range of 10-25%, 36-81% and 7.5-54%, respectively.

Subsequently, the simplex lattice design method was used to optimize the formulation of SE-OPEO. The experimental results are shown in **Table S1**. Design Expert 8.0.6 software was used to fit the data in **Table S1**. The following response equations (**Eq. 1** and **Eq. 2**) are obtained by model fitting with

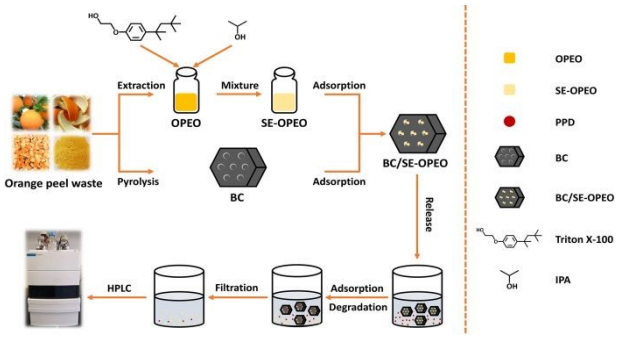


**Scheme 1** Preparation of BC/SE-OPEO and the adsorption and degradation of PPD.

**Table 1** Visual grading results of self-emulsifying efficiency [a]

| Oil | Surfactant | Co-surfactant | Grades |
|---|---|---|---|
| OPEO | Tween 20 | EtOH | C |
| | | IPA | C |
| | | PEG 400 | C |
| | Tween 80 | EtOH | C |
| | | IPA | C |
| | | PEG 400 | B |
| | Tween 85 | EtOH | C |
| | | IPA | C |
| | | PEG 400 | C |
| | Triton X-100 | EtOH | C |
| | | IPA | A |
| | | PEG 400 | B |

[a] Grading standards are listed in the section 1.3.1 of supplementary information.

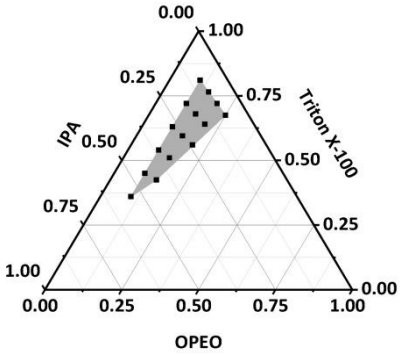


**Fig. 1** The pseudo-ternary phase diagram of OPEO, Triton X-100 and IPA.

the proportions of OPEO (A), Triton X-100 (B) and IPA (C) as independent variables, and average particle size ($Y_1$) and PDI ($Y_2$) as dependent variables:

$Y_1 = 279.74A + 12.10B + 75.15C - 48.13AB + 59.74AC - 173.31BC$
($R^2 = 0.9859$, $P < 0.0001$) **Eq. 1**

$Y_2 = 0.28A + 0.19B + 0.23C + 4.58 \times 10^{-3}AB - 0.09AC + 6.40 \times 10^{-3}BC$
($R^2 = 0.9662$, $P < 0.0001$) **Eq. 2**

The fitting effect of the mathematical model is determined by analyzing the R-Squared and P-value of regression equation. **Eq. 1** and **Eq. 2** show that the fitting effect of the model is good, and the representative model can predict objectively and accurately according to the independent variables. In the meanwhile, the two P-values are all less than 0.0001, demonstrating that the statistical level of the model is very significant. As such, **Eq. 1** and **Eq. 2** are suitable to optimize SE-OPEO formulation.

The contour plot diagrams and response surface diagrams were drawn (**Fig. 2**) according to the **Eq. 1** and **Eq. 2**. OPEO has a great influence on the average particle size. With increasing OPEO concentration, the average particle size also increases, and the trend is clear (**Fig. 2**). Moreover, the effect of Triton X-100 on the average particle size is stronger than that of IPA. The higher the concentration of Triton X-100 and IPA, the smaller the average particle size. This is because when the concentration of OPEO increases (or the concentration of Triton

View Article Online
DOI: 10.1039/D3GC00707C

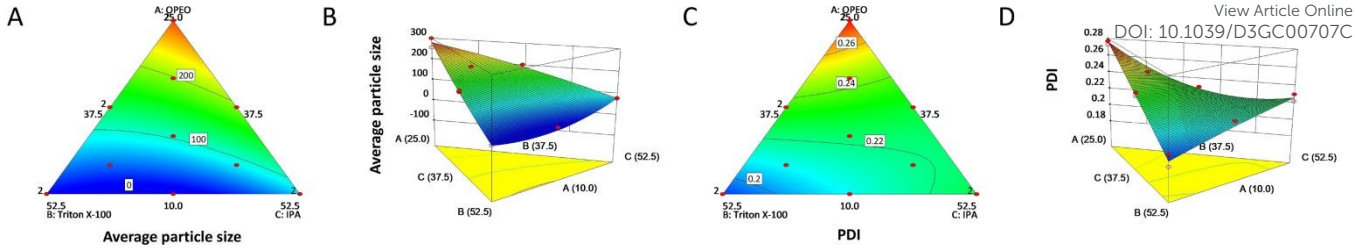


**Fig. 2** Contour plot diagram and response surface diagram for average particle size (A, B), PDI (C, D) as a function of OPEO, Triton X-100 and IPA.

X-100 reduces), the oil droplets will not be emulsified completely, resulting in an increase of interfacial tension and the formation of larger oil droplets.[17] Meanwhile, OPEO and Triton X-100 have a similar level of impact on polydispersity (PDI), but exhibit opposite impact trends. The effect of IPA on PDI is not obvious.

It was found that the smaller the average particle size of the emulsion, the larger the specific surface area,[18] and the smaller the PDI, the more uniform the particle size distribution.[19] Hence, the minimum average particle size and minimum PDI were set as constraints. The optimal formulation of SE-OPEO was determined to be OPEO/Triton X-100/IPA (10/52.5/37.5, w/w/w), and the average particle size and PDI were predicted to be 12.10 nm and 0.192, respectively. After that, three batches of SE-OPEO were prepared according to the optimal formulation predicted by Design Expert 8.0.6 software, and their average particle size and PDI was measured. The results are listed in **Table 2**. The deviations of average particle size and PDI are 0.41% and -1.04% respectively, denoting that the mathematical model has a good predictive effect.

BC was used to adsorb SE-OPEO to obtain BC/SE-OPEO with suitably greasy appearance and good flowability. The yields of BC obtained under different pyrolysis temperatures and times are shown in **Table 3**. With increasing pyrolysis temperature and time, the yield decreases. Moreover, the final weight of sample shows a large loss because of the loss of volatile components from the breakdown of the constituent polysaccharides and lignin.[20]

**Table 2** The predicted and experimental values of the optimal proportion [a]

| Indicators | Average particle Size (nm) | PDI |
|---|---|---|
| Predicted Value | 12.10 | 0.192 |
| Experimental Value | 12.05 ± 0.511 | 0.194 ± 0.004 |
| Bias (%) | 0.41 | -1.04 |

[a] Bias (%) = (predicted value - experimental value)/predicted value × 100; Values are presented as the mean ± SD (n=3).

**Table 3** The preparation conditions and yields of BC

| Pyrolysis Temperature (°C) | Pyrolysis Time (h) | Yield (%) |
|---|---|---|
| 900 | 3 | 11.65 |
| 1000 | 3 | 9.52 |
| 1100 | 3 | 6.19 |
| 1000 | 2 | 13.43 |
| 1000 | 4 | 6.48 |

**Characterization of the prepared materials**

The morphology of BC and BC/SE-OPEO was studied by Scanning electron microscopy (SEM) and Transmission electron microscopy (TEM) (**Fig. 3**). The SEM images of BC and BC/SE-OPEO are illustrated in **Fig. 3A** and **Fig.3B** respectively, where BC shows a rougher surface than BC/SE-OPEO. According to the TEM images of BC and BC/SE-OPEO (**Fig. 3C, D**), the appearance of BC/SE-OPEO is smoother than that of BC. These results indicate indirectly that BC is successfully loaded with SE-OPEO.

Gas chromatography-mass spectrometer (GC-MS) was used to identify the compositions of OPEO. As shown in **Fig. 4**, compound with retention time of around 3.7 min is limonene. The mass spectrum of limonene is illustrated in **Fig. S1**, including 41, 53, 68, 79, 93, 107, 121, 136 MS fragment peaks, the result is consistent with reported reference[21] (compound with retention time of around 2.5 min is solvent). Based on **Fig. 4**, limonene is the largest component of OPEO. In addition, 34 compositions of OPEO are founded except limonene, including terpenoid, aldehyde, alcohol, ester, ketone, acid, alkene and alkane compounds **(Table S2)**.

Characterization of functional groups in the prepared materials was conducted by Fourier transform infrared spectrometer (FT-IR) (**Fig. 5**). Limonene is the largest component in OPEO and dominates the spectra.[22] The characteristic bands in the FTIR spectra are: 3083 $cm^{-1}$ and 3010 $cm^{-1}$ (=C-H stretching vibrations), 2964 $cm^{-1}$ and 2917 $cm^{-1}$ (C-H

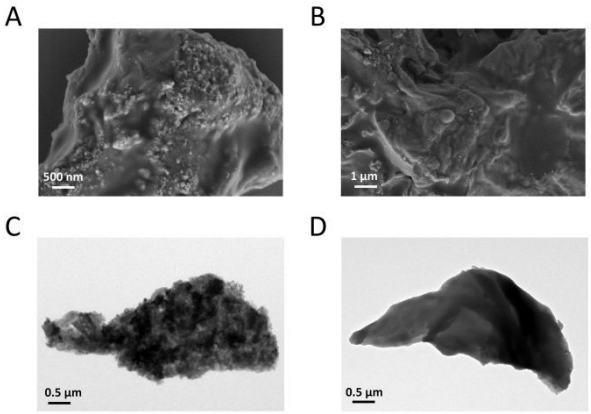


**Fig. 3** The SEM and TEM of BC and BC/SE-OPEO, where A, B, C, D stands for SEM of BC, SEM of BC/SE-OPEO, TEM of BC and TEM of BC/SE-OPEO, respectively.

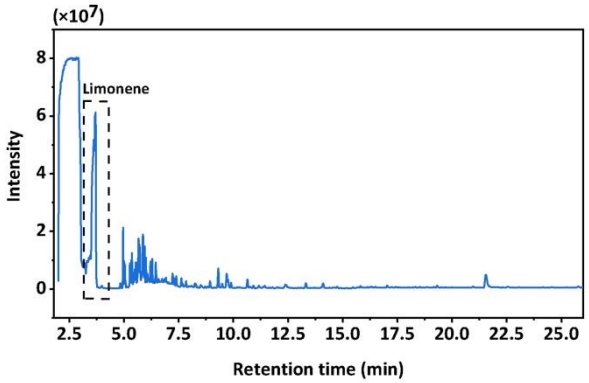


**Fig. 4** GC-MS of OPEO.

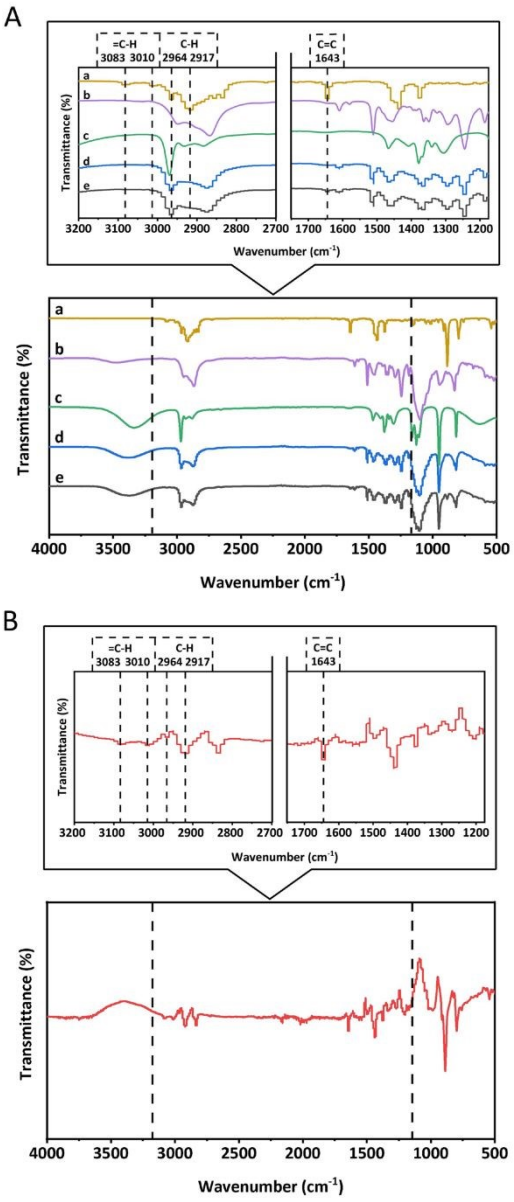


**Fig. 5** A: FT-IR spectra of OPEO (a), Triton X-100 (b), IPA (c), blank SE-OPEO (d), SE-OPEO (e); B: FT-IR spectral subtraction between SE-OPEO Fig. 5A (e) and blank SE-OPEO Fig. 5A (d).

stretching vibrations), 1643 $cm^{-1}$ (C=C stretching vibrations) of ring and vinyl group (**Fig. 5A, Curve a**).[23] **Fig. 5A, Curve b and c** show the FT-IR spectra of Triton X-100 and IPA, and **Curve d of Fig. 5A** is of blank SE-OPEO (only Triton X-100 and IPA). Although the characteristic band at 1643 $cm^{-1}$ (C=C stretching vibrations) appears in FT-IR spectrum of SE-OPEO (**Fig. 5A, Curve e**), most of the typical absorption peaks of limonene are covered up by the absorption peaks of Triton X-100 and IPA. To solve this problem, characteristic bands of OPEO were observed by spectral subtraction[23] (the FT-IR spectrum of SE-OPEO minus blank SE-OPEO is OPEO) (**Fig. 5B**), providing evidence of the presence of OPEO in SE-OPEO.

**Fig. 6** is the High-performance liquid chromatography (HPLC) chromatograms of limonene, OPEO, SE-OPEO, BC/SE-OPEO, blank SE-OPEO (only Triton X-100 and IPA) and blank BC/SE-OPEO (BC only loaded with Triton X-100 and IPA). Compound with retention time of around 7.3 min in the chromatograms of OPEO, SE-OPEO and BC/SE-OPEO is limonene according to the chromatogram of limonene (**Fig. 6, Curve a**), providing evidence that BC was successfully loaded with SE-OPEO.

The X-ray diffraction (XRD) patterns of BC and BC/SE-OPEO in the range from 5° to 90° are illustrated in **Fig. 7A**. In the XRD of BC, the broad diffraction peaks at 2θ=22° and 43° correspond to the (002) and (100) facets of amorphous carbon.[24] After BC was loaded with SE-OPEO, the same broad diffraction peaks appeared in the XRD patterns of BC/SE-OPEO, with no new peaks suggesting that the structure of BC is not destructed in the process of BC/SE-OPEO preparation. Thermogravimetric analysis (TGA) curves of corresponding species in this research are displayed in **Fig. 7B**, which indirectly demonstrates the successful preparation of BC/SE-OPEO.

Powder flowability is of great significance for detecting the content uniformity of SE-OPEO in BC. Generally, powders with an angle of repose of less than 40° are considered to satisfy the requirement of liquidity in industrial production.[25] It is widely believed that lower Hausner's ratio (HR) and Carr's index (CI) on behalf of freer flowability.[17] HR and CI no more than 1.25 and 21, respectively, proving that the powders have good flowability and are applicable to industrial production.[26] The angle of repose, HR and CI of BC/SE-OPEO are listed in **Table 4**. The results of the three parameters all conform to the above demands and as such it is considered that the prepared BC/SE-OPEO possesses good fluidity.

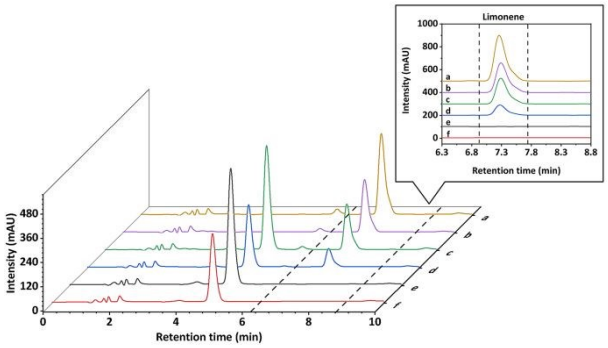


**Fig. 6** HPLC chromatograms of limonene (a), OPEO (b), SE-OPEO (c), BC/SE-OPEO (d), blank SE-OPEO (e) and blank BC/SE-OPEO (f).

View Article Online
DOI: 10.1039/D3GC00707C

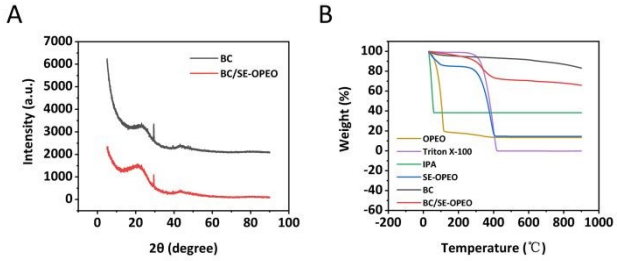


**Fig. 7** A: XRD patterns of BC and BC/SE-OPEO; B: TGA diagram of OPEO, Triton X-100, IPA, SE-OPEO, BC and BC/SE-OPEO.

**Table 4** The flowability of BC/SE-OPEO [a]

| Angle of Repose | HR | CI |
|---|---|---|
| 36.74 ± 0.56 | 1.17 ± 0.02 | 14.33 ± 1.53 |

[a] Values are presented as the mean ± SD (n=3).

### Adsorption and degradation of PPD by BC/SE-OPEO

The effects of BC pyrolysis temperature, BC pyrolysis time, BC/SE-OPEO dosage, contact time, contact temperature as well as solution pH on PPD adsorption and degradation were investigated. As is evident in **Fig. 8A**, with increasing BC pyrolysis temperature, the removal of PPD firstly increases and then decreases, and the removal efficiency reaches the highest values at pyrolysis temperature of 1000 °C, which is selected as the optimal pyrolysis temperature. Pyrolysis time has a similar impact on the removal of PPD (**Fig. 8B**), and the optimal pyrolysis time is 3 h. It is worth noting that as the pyrolysis temperature and pyrolysis time continue to increase, the removal efficiency of PPD decreases. The phenomenon can be due to the collapse of BC pores thus reducing the specific surface area of BC.

The effect of BC/SE-OPEO dosage on PPD removal is shown in **Fig. 8C**. The removal efficiency of PPD increases with increasing dosage due to the acquisition of additional pores and active sites on the materials for PPD adsorption and degradation: 50 mg was chosen as the optimal dosage. Subsequently, the contact time was explored (**Fig. 8D**), and 110 min is the optimal contact time. The influence of contact temperature on PPD removal is exhibited in **Fig. 8E**, and 40 °C was selected as the ideal contact temperature. The influence of solution pH on PPD removal is not significant (**Fig. 8F**) and BC/SE-OPEO can effectively adsorb and degrade PPD over a wide pH range.

The PPD removal efficiency can reach around 98% with 50 mg BC/SE-OPEO (BC pyrolyzed at 1000 °C for 3 h) after 110 min at 40 °C.

### Analysis of actual samples

To study the application ability of BC/SE-OPEO in real samples, BC/SE-OPEO was used to conduct adsorption and degradation on actual hair dye sewage and dyed hair samples under the optimal conditions. The overall HPLC chromatogram is shown in **Fig. S2**, and the HPLC chromatogram is illustrated in **Fig. 9**. The retention time of PPD is around 5.5 min according to the chromatogram of PPD standard (**Fig. 9, Curve a**). The concentration of PPD detected in the hair dye sewage sample is 22.03 mg/L and the removal efficiency of PPD can reach 99.26% after being treated with BC/SE-OPEO. The concentration of PPD in the dyed hair is 151.36 μg/g and the PPD removal efficiency can be up to 96.87%. These results prove that a) BC/SE-OPEO is suitable for hair dye sewage treatment and b) it has the potential for the application in hair protection after hair dyeing. The toxicology and other parameters of BC/SE-OPEO still need to be investigated in future research.

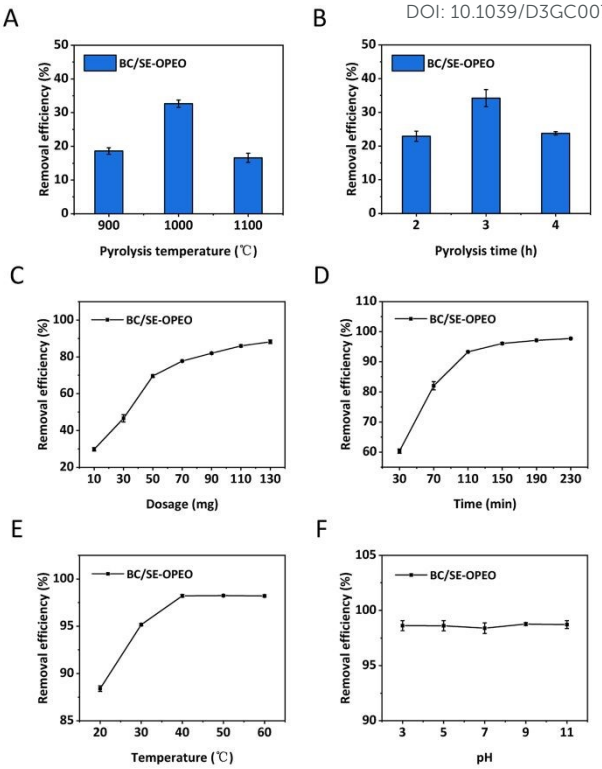


**Fig. 8** Effects of BC pyrolysis temperature (A), BC pyrolysis time (B) for PPD removal efficiency (single factor investigation of materials); effects of BC/SE-OPEO dosage (C), contact time (D), contact temperature (E) and solution pH (F) for PPD removal efficiency (single factor investigation of external influence). The error bars are the standard deviation of three parallel experiments.

### Scavenging experiments of ROS

To confirm the presence of ROS during the degradation of PPD, L-glutathione reduced (GSH) and ascorbic acid (ASC) as common ROS scavengers were used. The results are shown in **Fig. 10A**. The addition of GSH and ASC can inhibit the degradation of PPD, demonstrating that the presence of ROS and its key role in PPD degradation. In addition, it has reported that limonene is the causative substances for production of ROS.[16] This is the reason of OPEO can promote the production of ROS to degrade PPD.

View Article Online
DOI: 10.1039/D3GC00707G

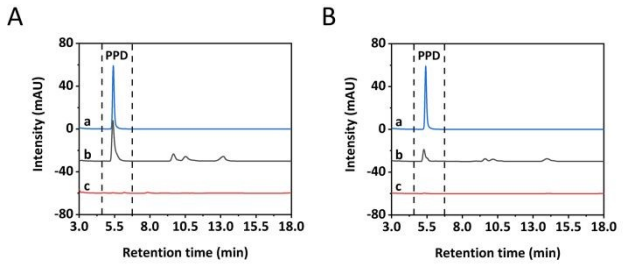


**Fig. 9** A: The HPLC chromatograms of PPD standard (a), hair dye sewage sample (b), hair dye sewage sample treated with BC/SE-OPEO (c); B: The HPLC chromatograms of PPD standard (a), dyed hair extraction sample (b), dyed hair sample treated with BC/SE-OPEO (c).

**Degradation intermediates and pathways**

Organic pollutants can be degraded to carbon dioxide and water by ROS with some intermediates forming during the process. Therefore, it is important to identify the intermediates produced in the reaction. High performance liquid chromatography-mass spectrometer (HPLC-MS) was used to identify the intermediates produced in samples of OPEO reacted with PPD in aqueous solution (**Fig. S3**). According to the intermediates detected in this research and previous literature[9], possible degradation pathways are proposed (**Fig. 10B**). These findings confirmed that the oxidation and attack of ROS would lead to the rapid decomposition of the ring structure during the degradation process.

## Conclusions

In this research, a novel BC/SE-OPEO material was prepared and used for adsorption and degradation of PPD. The results show that the optimal formulation of SE-OPEO is determined as OPEO/Triton X-100/IPA=10/52.5/37.5 (w/w/w), and the BC/SE-OPEO prepared subsequently has good flow performance. Furthermore, the results of SEM, TEM, GC-MS, FT-IR, HPLC and TGA prove that SE-OPEO and BC/SE-OPEO were successfully prepared, and XRD shows that the structure of BC is not damaged during the process of BC/SE-OPEO preparation. Adsorption and degradation experiments demonstrate that PPD removal efficiency of BC/SE-OPEO can reach around 98% under the optimal conditions. BC/SE-OPEO was then proved to be suitable for the removal of toxic PPD in hair dye sewage and dyed hair. Exploration of the mechanism reveals that OPEO can promote the production of ROS, so that PPD is ultimately degraded to carbon dioxide and water because the attack of ROS. The preparation and application of materials are all in line with green chemistry in this research. In summary, this work provides a successful, promising and environmentally friendly research strategy for pollutants degradation and shows a very useful application for a very large volume waste.

## Conflicts of interest

There are no conflicts to declare.

## Acknowledgements

This work was financially supported by National Natural Science Foundation of China (81973451, 22208036), Fundamental and Frontier Research Fund of Chongqing (CSTC2018JCYJAX0661, CSTC2019JSYJ-YZYSBAX0020), the Science and Technology Research Program of Chongqing Municipal Education Commission (KJZD-K201800103), Fundamental Research Funds for the Central Universities (2019CDYGYB027, 2022CDJXY-003), Graduate Research and Innovation Foundation of Chongqing (CYS18033), Graduate Research and Innovation Project of Chongqing (CYB22041), Venture & Innovation Support Program for Chongqing Overseas Returnees.

## Notes and references

1 A. Meyer and K. Fischer, *Environ. Sci. Eur.*, 2015, **27**, 11.
2 M. H. Al-Enezi and F. S. Aldawsari, *Cosmetics*, 2022, **9**, 41.
3 H. Woo, H. Kim, S. Shin, J. H. Shin, D. Ryu, D. Park and E. Jung, *Toxicol Rep*, 2021, **8**, 96-105.
4 M. C. Yu, P. L. Skipper, S. R. Tannenbaum, K. K. Chan and R. K. Ross, *Mutat. Res.*, 2020, **506–507**, 21–28.
5 S. A. Saleh Mahmud, T. Ferdous, M. M. Alam, M. S. Hossain, H. B. Shozib, F. Khalil, F. Akter and M. N. Hossain, *BRC*, 2021, **8**, 1088-1092.

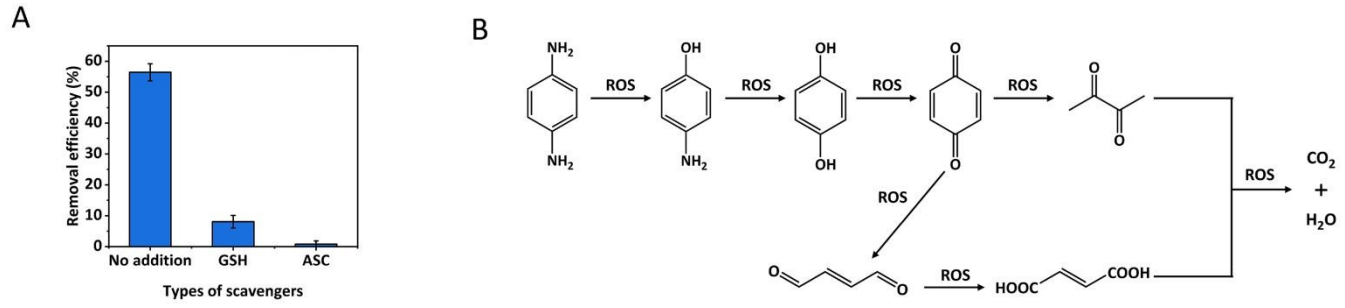


**Fig. 10** A: PPD removal efficiency in the presence of scavengers; B: Possible degradation pathways of PPD. The error bars are the standard deviation of three parallel experiments.

View Article Online
DOI: 10.1039/D3GC00707C

6 G. M. Elmanfe, O. E. Khreit, O. A. Abduljalil and N. M. Abbas, *Al-Mukhtar J. Sci.*, 2022, **37**, 13-21.
7 M. Devi, *Int J Res Anal Rev*, 2016, **3**, 19-23.
8 C. Dong, W. Fang, Q. Yi and J. Zhang, *Chemosphere*, 2022, **308**, 136205.
9 E. Asgari, A. Sheikhmohammadi, M. Mohammadian Fazli, R. Aali and F. Mohammadi, *Int. J. Environ. Anal. Chem*., 2022, DOI: 10.1080/03067319.2022.20781981-20.
10 Y. H. Chen, Y. Y. Liu, R. H. Lin and F. S. Yen, *J. Hazard. Mater*., 2009, **163**, 973-981.
11 L. Qiao, Y. Shi, Q. Cheng, B. Liu and J. Liu, *J. Water Reuse Desalin*., 2021, **11**, 212-223.
12 H. Yu, S. Yu, C. Ren and Z. Xiu, *Plasma Sci. Technol*., 2012, **14**, 157-161.
13 Y. Sunohara, K. Nakano, S. Matsuyama, T. Oka and H. Matsumoto, *Sci. Hortic*., 2021, **289**, 110493.
14 N. Ahuja, H. P. Singh, D. R. Batish and R. K. Kohli, *Pestic. Biochem. Physiol*., 2015, **118**, 64-70.
15 S. Dahiya, D. R. Batish and H. P. Singh, *Braz. J. Bot*., 2020, **43**, 447-457.
16 Y. Ao, K. Satoh, K. Shibano, Y. Kawahito and S. Shioda, *J. Clin. Biochem. Nutr*., 2008, **43**, 6-12.
17 J. Huang, Q. Wang, R. Sun, T. Li, N. Xia and Q. Xia, *J. Food Eng*., 2018, **226**, 22-30.
18 G. Chen and J. Wen, *J. Biomed.*, 2018, **3**, 50-59.
19 H. Zheng, J. Wang, Y. Zhang, Q. Xv, Q. Zeng and J. Wang, *Nanomaterials (Basel)*, 2022, **12**, 2189.
20 Y. Wang, S. L. Wang, T. Xie and J. Cao, *Bioresour. Technol*., 2020, **316**, 123929.
21 L. Yang, A. Nuerbiye, P. Cheng, J. H. Wang and H. Li, *Molecules*, 2017, **22**, 1790.
22 H. S. El-Beltagi, N. S. Eshak, H. I. Mohamed, E. S. A. Bendary and A. W. Danial, *Plants (Basel)*, 2022, **11**, 1740.
23 S. Mallardo, V. De Vito, M. Malinconico, M. G. Volpe, G. Santagata and M. L. Di Lorenzo, *Eur. Polym. J*., 2016, **79**, 82-96.
24 K. K. Beltrame, A. L. Cazetta, P. S. C. de Souza, L. Spessato, T. L. Silva and V. C. Almeida, *Ecotoxicol. Environ. Saf*., 2018, **147**, 64-71.
25 A. He, L. Liu, H. Yu and Y. Liu, *IOP Conf. Ser.: Earth Environ. Sci.*, 2020, **514**, 052003.
26 D. Wang, Y. Ma, Q. Wang, J. Huang, R. Sun and Q. Xia, *J. Food Sci*., 2019, **84**, 936-945.